

REVISITING THE JONES EIGENPROBLEM IN FLUID-STRUCTURE INTERACTION*

SEBASTIAN DOMINGUEZ[†], NILIMA NIGAM[†], AND JIGUANG SUN[‡]

Abstract. The Jones eigenvalue problem first described in [15] concerns unusual modes in bounded elastic bodies: time-harmonic displacements whose tractions and normal components are both identically zero on the boundary. This problem is usually associated with a lack of unique solvability for certain models of fluid-structure interaction. The boundary conditions in this problem appear, at first glance, to rule out *any* non-trivial modes unless the domain possesses significant geometric symmetries. Indeed, Jones modes were shown to not be possible in most C^∞ domains in [7]. However, we show in this paper that while the existence of Jones modes sensitively depends on the domain geometry, such modes *do* exist in a broad class of domains. This paper presents the first detailed theoretical and computational investigation of this eigenvalue problem in Lipschitz domains. We also analytically demonstrate Jones modes on some simple geometries.

Key words. fluid-structure interaction, Jones eigenvalue problem, finite element method

AMS subject classifications. 65N25, 65N30, 74B05

1. Introduction. In this paper we investigate the *Jones eigenvalue problem*, which is to locate non-trivial $\mathbf{u} \in \mathbb{R}^n$, $n \in \{2, 3\}$, and $w \in \mathbb{C}$ so that

$$\begin{aligned} (1a) \quad \mathcal{L}\mathbf{u} &:= -(\mu\Delta\mathbf{u} + (\lambda + \mu)\nabla(\operatorname{div}\mathbf{u})) = -\rho w^2\mathbf{u} && \text{in } \Omega, \\ (1b) \quad &(\mu\nabla\mathbf{u})(\lambda + \mu)(\operatorname{div}\mathbf{u})\mathbf{I}\mathbf{n} = \mathbf{0} && \text{on } \partial\Omega, \\ (1c) \quad &\mathbf{u} \cdot \mathbf{n} = 0 && \text{on } \partial\Omega. \end{aligned}$$

Here $\Omega \subseteq \mathbb{R}^n$ is a bounded domain with Lipschitz boundary $\partial\Omega$, \mathbf{n} is the unit outer normal on $\partial\Omega$, $\rho > 0$ is a *density* and $\mu > 0$, $\lambda \in \mathbb{R}$ such that $\lambda + (\frac{2}{n})\mu > 0$ are the so-called *Lamé parameters*.

The Jones eigenvalue problem arises when studying time-harmonic solutions of a fluid-solid interaction problem in \mathbb{R}^n . Precisely, suppose an isotropic elastic bounded body occupying region Ω is immersed in an inviscid compressible fluid occupying the rest of the space. The Jones eigenvalue problem coincides exactly with determination of non-trivial solutions of the corresponding homogeneous equations governing the displacements of the elastic body. The occurrence of these eigenpairs was first noticed in [15], where the author introduced the fluid-solid interaction problem of interest and pointed out this lack of uniqueness in the fluid-structure problem. Many other authors have noticed this non-uniqueness issue in this model [2, 4, 9, 10, 11, 13, 18, 20, 22]. In these papers the main interest was in studying the full fluid-structure problem, and the Jones eigenmodes were of interest only within the context of well-posedness, which was only guaranteed in away from such modes. We note this is not the only possible model for fluid-structure interaction in the frequency domain; other models which ameliorate the breakdown of uniqueness at exceptional frequencies have been proposed. We discuss this later [section 2](#).

*Submitted to the editors DATE.

Funding: This work was partially supported by CONICYT-Chile through Becas Chile, NSERC through the Discovery program, and NSF DMS-1521555.

[†]Department of Mathematics, Simon Fraser University, Burnaby, BC (domingue@sfu.ca, nigam@math.sfu.ca).

[‡]Department of Mathematical Sciences, Michigan Technological University, MI (jiguangs@mtu.edu)

Our focus in this paper is the eigenvalue problem [Equation 1](#), which possesses truly interesting features. We notice that [Equation 1a](#) and [Equation 1b](#) together define a standard eigenvalue problem (we call this the *traction eigenvalue problem*) for the Lamé operator \mathcal{L} on Ω , analogous to the Neumann eigenvalue problem for the Laplacian.

The traction eigenvalue problem has been extensively studied and has numerous applications in mechanical engineering; the existence of a countable discrete spectrum for Lipschitz domains is well-established (see, e.g. [\[16\]](#)). However, the problem under consideration in the present article asks: do there exist traction eigenmodes which additionally satisfy [Equation 1c](#)? This constraint intimately couples the geometry of the domain with the Jones eigenmode; in essence, the only traction modes which are also Jones modes are those which are purely tangential to the boundary.

Not much is known about the Jones eigenvalue problem itself. As mentioned, the most intriguing feature of this problem is its dependence on the boundary of the domain. An influential paper [\[7\]](#) shows that for almost any 3D domain with C^∞ boundary, there can be no modes with free traction and zero normal component on the boundary that solve the Jones eigenvalue problem. The central claim in this paper was established in a fairly narrow setting - for instance, the analysis cannot extend to domains with corners - yet perhaps the main theorem served to deter further investigations. Likewise, [\[21\]](#) shows that smooth 3D domains having two flat non-parallel manifolds of the boundary cannot support a non-trivial divergence-free mode. Even though the authors claim these kind of deformations are Jones eigenvectors, we note that the full eigenproblem [Equation 1a](#) does not impose the condition on the divergence. Therefore, the result in [\[21\]](#) is only excludes a subset of possible Jones modes.

The rest of this paper is organized as follows: in [section 2](#) we introduce the eigenvalue problem. We first describe the fluid-solid interaction where the Jones modes appear. We provide exact Jones eigenmodes on rectangles. We next provide a detailed description of the point spectrum of this problem and identify important properties relating the eigenpairs with the domain. In [section 3](#) we derive a primal formulation to approximate Jones eigenpairs where the extra constraint on the displacement in the normal direction on the boundary has been introduced as an essential condition in the search and test spaces. The continuity of the normal trace will ensure this space is closed. A careful treatment of this formulation is then provided as it is known that the spectrum of this problem depends heavily on the geometry of the domain [\[7, 21\]](#). In fact, the proof of the usual ellipticity of one of the bilinear forms depends entirely on a Korn's inequality shown in [\[3\]](#) for Lipschitz domains in \mathbb{R}^n , with $n \in \{2, 3\}$. A weaker version of this result for domains with C^1 boundary is given in [\[5\]](#). In addition, in [\[3\]](#) the authors showed that the gradient of a vector with mixed tangential and/or normal components vanishing on the boundary can be bounded (up to a constant) above by the deviatoric part of its strain tensor in concave or polyhedral domains in \mathbb{R}^3 with piecewise C^2 boundaries (as defined in the same reference). In [section 4](#) we develop a conforming discretization of the continuous eigenvalue problem via Lagrange finite elements. Finally, some numerical results showing the good performance of our method on polyhedral domains are presented in [section 5](#).

The sensitivity of the spectrum to the shape of the domain suggests that the classical FEM using triangular meshes may not be the best method to use to approximate the spectrum of this problem for curved domains. Numerical examples presented show the performance of the proposed scheme and exhibit the different regularity of the eigenfunctions of this problem in different domains.

2. The interaction problem. Solutions of the Jones eigenvalue problem appear as non-trivial elements in the kernel of a model of fluid-solid interaction where an isotropic elastic body is immersed in an inviscid fluid occupying the whole space \mathbb{R}^n , $n \in \{2, 3\}$. In this section we introduce such problem and establish its connection with the Jones eigenpairs.

2.1. Some notation. We begin by fixing notation for the remainder of this paper. For vectors in \mathbb{R}^n , the operation $\mathbf{a} \cdot \mathbf{b}$ is the standard dot product with induced norm $\|\cdot\|$. For second-order tensors $\boldsymbol{\sigma}, \boldsymbol{\tau}$ in $\mathbb{R}^{n \times n}$, the double dot product is the usual Frobenius inner product for matrices

$$\boldsymbol{\sigma} : \boldsymbol{\tau} := \sum_{i,j=1}^n \tau_{ij} \sigma_{ij} = \text{tr}(\boldsymbol{\tau}^t \boldsymbol{\sigma}).$$

This inner product induces the usual Frobenius norm. For differential operators, ∇ denotes the usual gradient operator acting of either a scalar field or a vector field. The divergence operator “div” of a vector field reduces to the trace of its gradient. The operator “**div**” acting on tensors stands for the usual divergence operator applied to each row of the tensors. The deviatoric part of a tensor of $\boldsymbol{\tau}$ is $\boldsymbol{\tau}^d := \boldsymbol{\tau} - \frac{1}{n} \text{tr}(\boldsymbol{\tau}) \mathbf{I}$, where \mathbf{I} is the identity matrix of $n \times n$ entries. If $\boldsymbol{\tau}, \boldsymbol{\sigma}$ are second-order tensors whose entries are $L^2(\Omega)$ functions on a bounded domain Ω , we define

$$(\boldsymbol{\tau}, \boldsymbol{\sigma})_0 := \int_{\Omega} \boldsymbol{\tau} : \boldsymbol{\sigma} \, d\Omega.$$

We observe that

$$\|\boldsymbol{\tau}^d\|_0^2 = \|\boldsymbol{\tau}\|_0^2 - \frac{2}{n} (\text{tr}(\boldsymbol{\tau}) \mathbf{I}, \boldsymbol{\tau})_0 + \frac{1}{n^2} (\text{tr}(\boldsymbol{\tau}) \mathbf{I}, \text{tr}(\boldsymbol{\tau}) \mathbf{I})_0 = \|\boldsymbol{\tau}\|_0^2 - \frac{1}{n} \|\text{tr}(\boldsymbol{\tau})\|_0^2.$$

If $\mathbf{u} \in \mathbb{R}^n$, the strain tensor tensor is a symmetric second-order tensor

$$\boldsymbol{\varepsilon}(\mathbf{u}) := \frac{1}{2} (\nabla \mathbf{u} + (\nabla \mathbf{u})^t).$$

Finally, if $\mathbf{u} := F(x, y) \hat{i} + G(x, y) \hat{j} \in \mathbb{R}^2$, we denote the two-dimensional rot by $\text{rot } \mathbf{u} := \frac{\partial G}{\partial x} - \frac{\partial F}{\partial y}$.

2.2. Fluid-solid interaction problem. As discussed in [section 1](#), the Jones eigenproblem was originally described within the context of a fluid-structure interaction problem. Consider a bounded, simply connected domain $\Omega_s \subseteq \mathbb{R}^n$ with boundary $\Gamma_s := \partial\Omega_s$ representing an isotropic linearly elastic body in \mathbb{R}^n . This body is assumed to be immersed in a compressible inviscid fluid occupying the region $\Omega_f := \mathbb{R}^n \setminus \bar{\Omega}_s$. See [Figure 1](#) for a schematic of this situation. Note that the bounded part of the boundary of Ω_f , $\Gamma_f := \partial\Omega_f$ coincides with the boundary of the (bounded region) Ω . For simplicity we write $\Gamma := \Gamma_f = \Gamma_s$.

The parameters describing the elastic properties of Ω_s are the so-called Lamé constants $\mu > 0$ and $\lambda \in \mathbb{R}$, satisfying the condition

$$(2) \quad \lambda + \left(\frac{2}{n}\right) \mu > 0$$

One fluid-structure interaction problem of interest concerns the situation when the fields are time-harmonic, allowing us to factor out the time-dependence and consider

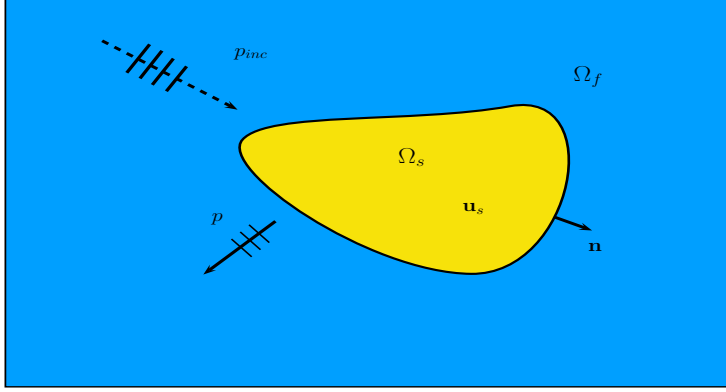


FIG. 1. Schematic of fluid-structure interaction problem.

the problem in the frequency domain. Using standard interface conditions coupling the pressure in the fluid p and the elastic displacement in the solid \mathbf{u} , the fluid-solid interaction problem in the frequency domain reads: given volumetric forces \mathbf{f} and \mathbf{g} , and an incident pressure p_{inc} , find a pressure field p in Ω_f and elastic deformations \mathbf{u} of Ω_s , satisfying

$$(3a) \quad \Delta p + \left(\frac{w^2}{c^2}\right)p = \text{div } \mathbf{f}, \quad \text{on } \Omega_f, \quad -\rho w^2 \mathbf{u} - \text{div } \boldsymbol{\sigma}(\mathbf{u}) = \mathbf{g}, \quad \text{in } \Omega_s,$$

$$(3b) \quad -(p + p_{\text{inc}})\mathbf{n} = \boldsymbol{\sigma}(\mathbf{u})\mathbf{n}, \quad \frac{\partial}{\partial \mathbf{n}}(p + p_{\text{inc}}) = \rho w^2 \mathbf{u} \cdot \mathbf{n}, \quad \text{on } \Gamma,$$

$$(3c) \quad \frac{\partial p}{\partial r} - i\left(\frac{w}{c}\right)p = o(1/r), \quad \text{as } r := \|\mathbf{x}\| \rightarrow \infty.$$

The parameter c^2 is the constant speed of the sound in the fluid, and the Cauchy tensor $\boldsymbol{\sigma}$ depends on the Lamé constants $\mu > 0$ and $\lambda \in \mathbb{R}$ and is defined in terms of the strain tensor $\boldsymbol{\varepsilon}(\mathbf{u})$ as

$$\boldsymbol{\sigma}(\mathbf{u}) := 2\mu\boldsymbol{\varepsilon}(\mathbf{u}) + \lambda \text{tr}(\boldsymbol{\varepsilon}(\mathbf{u}))\mathbf{I}, \quad \text{in } \Omega_s.$$

Using the vector Laplacian operator, we see that

$$\text{div } \boldsymbol{\sigma}(\mathbf{u}) = \mu\Delta\mathbf{u} + (\lambda + \mu)\nabla(\text{div } \mathbf{u}) \quad \text{on } \Omega_s.$$

This is a commonly accepted formulation for time-harmonic fluid-solid interaction problems involving inviscid flow, see, for example, [11, 13, 14]. The system in Equation 3 is known to possess a non-trivial kernel under certain situations. As discussed in [15], this problem lacks a unique solution whenever \mathbf{u} is a non-trivial solution of the homogeneous problem:

$$(4) \quad -\text{div } \boldsymbol{\sigma}(\mathbf{u}) = \rho w^2 \mathbf{u}, \quad \text{in } \Omega_s, \quad \boldsymbol{\sigma}(\mathbf{u})\mathbf{n} = \mathbf{0}, \quad \mathbf{u} \cdot \mathbf{n} = 0, \quad \text{on } \Gamma.$$

The pair (w^2, \mathbf{u}) solving this eigenvalue problem is a Jones eigenpair [15]. The homogeneous problem for the displacements can be viewed as the usual eigenvalue problem for linear elasticity with traction free boundary condition, plus the extra constraint on the normal trace of \mathbf{u} along the boundary. Therefore, we may consider this as an overdetermined problem. We know that there is a countable number of eigenmodes

for linear elasticity with free traction given reasonable assumptions on Γ (see [1] and references therein). The extra condition $\mathbf{u} \cdot \mathbf{n} = 0$ on the boundary plays an important role in the existence of the zero eigenvalue of Equation 4. All of these properties are discussed in detail in the next sections.

A slightly different model for fluid-structure interaction in the frequency domain can be derived by considering the problem with non-zero fluid viscosity and then taking this to zero. We omit further details about this model and refer the reader to [11] for a detailed description of this case. As pointed out in [11], adding a condition on the shear of \mathbf{u} on the interface may be another fix for the non-uniqueness of Equation 3. The condition

$$\rho \omega^2 \mathbf{u} \cdot \mathbf{t} = \frac{\partial}{\partial \mathbf{t}} (\boldsymbol{\sigma}(\mathbf{u}) \mathbf{n} \cdot \mathbf{n}),$$

removes the non-zero solutions of (4). Here \mathbf{t} is the unit tangent vector on Γ . In [6], the authors add a Robin boundary condition for the fluid pressure on a far enough “artificial” boundary containing the solid. They then consider the fluid to be bounded between the solid and this interface. As shown in the same reference, this modified problem has a unique solution.

Since our interest in the present paper concerns the eigenvalue problem Equation 1, we do not delve any further into the properties of the interaction problem (cf. Equation 3).

In what follows we need to identify domains which are *axisymmetric*. We employ the definition given in [3]: The domain Ω is axisymmetric if it is invariant under rotations about an axis of symmetry. With this definition one can see that in the 2D case the circle and its complement are the only axisymmetric domains, with z as the axis of symmetry. For the 3D case, the number of axisymmetric domains becomes a lot larger. Any solid of rotation is axisymmetric, and has circular cross-section transverse to the axis of rotation.

2.3. Lipschitz domains can support Jones modes. The paper by Hargé in 1990 [7] examined the existence of non-trivial solutions of Equation 1. The results of this paper have been cited extensively in subsequent works focusing on the well-posedness of the fluid-structure model presented in the previous section. As an instance, “*Fortunately, these traction-free oscillations occur only in highly specific situations...*” [12]; “*Note that Hargé [...] has established that Jones modes do not exist for arbitrarily-shaped bodies.*” [2]; “*However, intuitively, we do not expect Jones frequencies to exist for an “arbitrary” body; this has been proved recently by Hargé [...]*”. [19] These papers also note that domains which are axisymmetric may indeed have such modes. As a historical aside, Horace Lamb [17] documented such modes in the sphere in 1881.

Revisiting [7], we note that the setting of the paper is as follows:

Pour Ω ouvert borné connexe de \mathbb{R}^3 à bord C^∞ ... fixé et soit $E = \left\{ \phi \in C^\infty(\overline{\Omega}; \mathbb{R}^3); \phi \text{ difféomorphisme de } \overline{\Omega} \text{ sur } \phi(\overline{\Omega}) \right\}$; on munit E de la topologie C^∞ ...[7]

and the main theorem is then

There is a open, countable dense intersection G of open sets of E such that for any ϕ in G , there is no exceptional eigenvalue ...[7]

This theorem and its technique of proof cannot be directly applied to the situation of polygonal domains in \mathbb{R}^2 , nor to polyhedral domains. Intuitively one may believe the result should hold in polygonal or polyhedral domains; indeed, our initial starting

point for the current study was to try to extend the result of Hargé to general Lipschitz domains, and hence to try to show the *converse* of the result we eventually establish in this paper. The critical observation was the following example.

It is easy to verify by inspection that $(w_s^2, \mathbf{u}_s), (w_p^2, \mathbf{u}_p)$ defined below are Jones eigenpairs on the rectangle $\Omega = [0, a] \times [0, b]$:

$$(5a) \quad \mathbf{u}_s = (a\ell) \sin\left(\frac{m\pi x}{a}\right) \cos\left(\frac{\ell\pi y}{b}\right) \hat{i} - (bm) \cos\left(\frac{m\pi x}{a}\right) \sin\left(\frac{\ell\pi y}{b}\right) \hat{j},$$

$$(5b) \quad w_s^2 = \frac{\mu\pi^2}{\rho} \left(\frac{m^2}{a^2} + \frac{\ell^2}{b^2} \right), \quad m, \ell = 1, 2, \dots,$$

and

$$(6a) \quad \mathbf{u}_p = (bm) \sin\left(\frac{m\pi x}{a}\right) \cos\left(\frac{\ell\pi y}{b}\right) \hat{i} + (a\ell) \cos\left(\frac{m\pi x}{a}\right) \sin\left(\frac{\ell\pi y}{b}\right) \hat{j},$$

$$(6b) \quad w_p^2 = \frac{(\lambda + 2\mu)\pi^2}{\rho} \left(\frac{m^2}{a^2} + \frac{\ell^2}{b^2} \right), \quad m, \ell = 0, 1, \dots, \quad m + \ell > 0.$$

It can also be readily seen that $\nabla \cdot \mathbf{u}_s = 0$ and $\text{rot } \mathbf{u}_p = 0$; eigenmodes of this form are termed *s*- and *p*- modes respectively. Further, some eigenvalues may have geometric multiplicity depending on $a(\cdot, \cdot)$ and b . In case $\lambda, \mu, \frac{a^2}{b^2} \in \mathbb{Q}$, provided we can find integer pairs (m, ℓ) and (n, k) satisfying

$$\frac{\mu\pi^2}{\rho} \left(\frac{m^2}{a^2} + \frac{\ell^2}{b^2} \right) = \frac{(\lambda + 2\mu)\pi^2}{\rho} \left(\frac{n^2}{a^2} + \frac{k^2}{b^2} \right) =: w^2,$$

the value w^2 is a higher-multiplicity Jones eigenvalue with an associated eigenspace which includes both *s*- and *p*- modes.

Studying this simple example, it became clear that the situation for polygonal domains required a different approach, and would yield different results, than for the setting in [7]. We can imagine, for example, that under certain conditions it could be possible for domains comprising a finite union of rectangles could possess Jones modes.

3. Weak formulation. In the presence of corners or edges, it is no longer reasonable to ask for the problem Equation 4 to be imposed pointwise, and a weak formulation is needed. Later in this paper we shall compute Jones modes using a finite element discretization.

Let Ω be a Lipschitz domain of \mathbb{R}^n (we drop the subscript referring to the solid domain). Recall the eigenvalue problem in Equation 4: find the Jones pairs (w^2, \mathbf{u}) , \mathbf{u} non-zero, such that

$$(7a) \quad -\text{div } \boldsymbol{\sigma}(\mathbf{u}) = \rho w^2 \mathbf{u}, \quad \text{in } \Omega,$$

$$(7b) \quad \boldsymbol{\sigma}(\mathbf{u})\mathbf{n} = \mathbf{0}, \quad \mathbf{u} \cdot \mathbf{n} = 0, \quad \text{on } \partial\Omega$$

with $\rho > 0$ a fixed constant. Using the definition of the Cauchy stress tensor, we can write Equation 7 as

$$(8a) \quad \mu \Delta \mathbf{u} + (\lambda + \mu) \nabla(\text{div } \mathbf{u}) + \rho w^2 \mathbf{u} = \mathbf{0} \quad \text{in } \Omega,$$

$$(8b) \quad (\mu \nabla \mathbf{u} + (\lambda + \mu)(\text{div } \mathbf{u})\mathbf{I})\mathbf{n} = \mathbf{0}, \quad \mathbf{u} \cdot \mathbf{n} = 0, \quad \text{on } \partial\Omega.$$

In order to introduce a weak formulation of [Equation 7](#) (equivalently [Equation 8](#)), we define the spaces

$$\mathbf{H}^1(\Omega) := \left\{ \mathbf{v} = (v_1, \dots, v_n) : v_i \in H^1(\Omega) \right\}, \quad \mathbf{H} := \left\{ \mathbf{u} \in \mathbf{H}^1(\Omega) : \gamma_{\mathbf{n}} \mathbf{u} = 0 \text{ on } \partial\Omega \right\}.$$

Here $H^1(\Omega)$ is the usual energy space for scalar-valued functions and $\gamma_{\mathbf{n}} : \mathbf{H}^1(\Omega) \rightarrow H^{-1/2}(\partial\Omega)$ is the normal trace operator, $\gamma_{\mathbf{n}}(\mathbf{v}) := (\mathbf{v} \cdot \mathbf{n})|_{\partial\Omega}$ for smooth \mathbf{v} . The space $H^{-1/2}(\partial\Omega)$ is defined as $H^{-1/2}(\partial\Omega) := (H^{1/2}(\partial\Omega))^*$, where $H^{1/2}(\partial\Omega)$ is the space of traces of elements in $H^1(\Omega)$. The space \mathbf{H} is endowed with the obvious \mathbf{H}^1 -inner product $(\cdot, \cdot)_1$. Note that the operator $\gamma_{\mathbf{n}}$ is continuous on $\mathbf{H}^1(\Omega)$ so that \mathbf{H} is a closed subspace of $\mathbf{H}^1(\Omega)$. We consider the following primal formulation of [Equation 8](#): find $\mathbf{u} \in \mathbf{H}$ and $\kappa \in \mathbb{C}$ such that

$$(9) \quad a(\mathbf{u}, \mathbf{v}) = \kappa \cdot (\mathbf{u}, \mathbf{v})_0, \quad \forall \mathbf{v} \in \mathbf{H},$$

where $\kappa := \rho w^2$, and the bilinear form $a : \mathbf{H} \times \mathbf{H} \rightarrow \mathbb{R}$ is given by

$$a(\mathbf{u}, \mathbf{v}) := \mu(\nabla \mathbf{u}, \nabla \mathbf{v})_0 + (\lambda + \mu)(\operatorname{div} \mathbf{u}, \operatorname{div} \mathbf{v})_0, \quad \forall \mathbf{u}, \mathbf{v} \in \mathbf{H}.$$

Since $\|\operatorname{div} \mathbf{u}\| \leq \|\nabla \mathbf{u}\| \leq \|\mathbf{u}\|_1$, for all $\mathbf{u} \in \mathbf{H}^1(\Omega)$, the bilinear form $a(\cdot, \cdot)$ is bounded. In addition, $a(\cdot, \cdot)$ is symmetric and positive semi-definite. We can define the Rayleigh quotient, and see that

$$(10) \quad \frac{a(\mathbf{v}, \mathbf{v})}{\|\mathbf{v}\|_0^2} \geq 0, \quad \forall \mathbf{v} \in \mathbf{H}, \mathbf{v} \neq \mathbf{0}.$$

We see that all possible eigenvalues of [Equation 9](#) are real and non-negative. Using the Cauchy tensor $\boldsymbol{\sigma}$ we can write [Equation 9](#) in the equivalent form

$$(11) \quad \tilde{a}(\mathbf{u}, \mathbf{v}) = \kappa \cdot (\mathbf{u}, \mathbf{v})_0, \quad \forall \mathbf{v} \in \mathbf{H},$$

where $\tilde{a}(\mathbf{u}, \mathbf{v}) := (\boldsymbol{\sigma}(\mathbf{u}), \nabla \mathbf{v})_0 = (\boldsymbol{\sigma}(\mathbf{u}), \boldsymbol{\varepsilon}(\mathbf{v}))_0$ for all $\mathbf{u}, \mathbf{v} \in \mathbf{H}$. In terms of the strain tensor only, $\tilde{a}(\cdot, \cdot)$ becomes

$$\tilde{a}(\mathbf{u}, \mathbf{v}) = 2\mu(\boldsymbol{\varepsilon}(\mathbf{u}), \boldsymbol{\varepsilon}(\mathbf{v}))_0 + \lambda(\operatorname{tr}(\boldsymbol{\varepsilon}(\mathbf{u})), \operatorname{tr}(\boldsymbol{\varepsilon}(\mathbf{v})))_0.$$

Using the deviatoric part of the strain tensor we can write

$$(12) \quad \tilde{a}(\mathbf{u}, \mathbf{v}) = 2\mu(\boldsymbol{\varepsilon}(\mathbf{u})^d, \boldsymbol{\varepsilon}(\mathbf{v})^d)_0 + \left(\lambda + \frac{2\mu}{n} \right) (\operatorname{tr}(\boldsymbol{\varepsilon}(\mathbf{u})), \operatorname{tr}(\boldsymbol{\varepsilon}(\mathbf{v})))_0, \quad \forall \mathbf{u}, \mathbf{v} \in \mathbf{H}.$$

Obviously, $a(\mathbf{u}, \mathbf{v}) = \tilde{a}(\mathbf{u}, \mathbf{v})$ for all $\mathbf{u}, \mathbf{v} \in \mathbf{H}$. Furthermore, the bilinear forms $a(\cdot, \cdot)$ and $\tilde{a}(\cdot, \cdot)$ are bounded in $\mathbf{H}^1(\Omega) \times \mathbf{H}^1(\Omega)$ and hence in $\mathbf{H} \times \mathbf{H}$. We can then define the solution operator $\tilde{T} : \mathbf{H} \rightarrow \mathbf{H}$ by $\tilde{T}\mathbf{f} = \mathbf{u}$ such that

$$(13) \quad \tilde{a}(\mathbf{u}, \mathbf{v}) = (\mathbf{f}, \mathbf{v})_0, \quad \forall \mathbf{v} \in \mathbf{H}.$$

If we can prove that \tilde{T} is a compact linear operator on \mathbf{H} , we are guaranteed that \tilde{T} has a countable point spectrum $\{\beta_n\} \subseteq (0, 1)$ and eigenfunctions $\{\mathbf{u}_n\}$ such that $\tilde{T}\mathbf{u}_n = \beta_n \mathbf{u}_n$ for all n . The corresponding eigenvalues of [Equation 11](#) would be $\kappa_n = \frac{1}{\beta_n}$, and \mathbf{u}_n would be the eigenfunctions.

It is clear from the properties of $\tilde{a}(\cdot, \cdot)$ that \tilde{T} is a linear and self-adjoint map from $\mathbf{H} \rightarrow \mathbf{H}$. We need to show that \tilde{T} is bounded and compact, which will rely on

the coercivity properties of $\tilde{a}(\cdot, \cdot)$. The positiveness of \tilde{a} will depend crucially on the domain shape as we shall see.

Using the definition of $\tilde{a}(\cdot, \cdot)$, we have

$$\begin{aligned} \tilde{a}(\mathbf{u}, \mathbf{u}) &= 2\mu \|\boldsymbol{\varepsilon}(\mathbf{u})^d\|_0^2 + \left(\lambda + \frac{2\mu}{n}\right) \|\text{tr}(\boldsymbol{\varepsilon}(\mathbf{u}))\|_0^2 \\ &= n \left(\frac{2\mu}{n} \|\boldsymbol{\varepsilon}(\mathbf{u})^d\|_0^2 + \left(\lambda + \frac{2\mu}{n}\right) \frac{1}{n} \|\text{tr}(\boldsymbol{\varepsilon}(\mathbf{u}))\|_0^2\right) \\ &\geq \min \left\{ 2\mu, n \left(\lambda + \frac{2\mu}{n}\right) \right\} \left(\|\boldsymbol{\varepsilon}(\mathbf{u})^d\|_0^2 + \frac{1}{n} \|\text{tr}(\boldsymbol{\varepsilon}(\mathbf{u}))\|_0^2 \right), \quad \forall \mathbf{u} \in \mathbf{H} \\ &= \min \left\{ 2\mu, n \left(\lambda + \frac{2\mu}{n}\right) \right\} \|\boldsymbol{\varepsilon}(\mathbf{u})\|_0^2, \quad \forall \mathbf{u} \in \mathbf{H}. \end{aligned}$$

where we have used $\|\boldsymbol{\tau}\|_0^2 = \|\boldsymbol{\tau}^d\|_0^2 + \frac{1}{n} \|\text{tr}(\boldsymbol{\tau})\|_0^2$. This establishes the inequality

$$(14) \quad \tilde{a}(\mathbf{u}, \mathbf{u}) \geq \min \left\{ 2\mu, n \left(\lambda + \frac{2\mu}{n}\right) \right\} \|\boldsymbol{\varepsilon}(\mathbf{u})\|_0^2, \quad \forall \mathbf{u} \in \mathbf{H}.$$

Now, $\kappa = 0$ will be an eigenvalue of [Equation 11](#) under certain conditions; this implies that $\tilde{a}(\cdot, \cdot)$ is not coercive on \mathbf{H} , and we cannot directly work with the solution map \tilde{T} to study the Jones spectrum in these cases. We defer the discussion of this situation to [subsection 3.2](#).

It turns out that for *non-axisymmetric Lipschitz domains*, $\kappa = 0$ is not in the point spectrum of [Equation 11](#). We establish this in the following subsection.

3.1. Existence of Jones modes on non-axisymmetric domains. Let Ω be a non-axisymmetric domain in \mathbb{R}^n , $n \in \{2, 3\}$. In [\[3\]](#), it was shown the following positivity bound for non-axisymmetric Lipschitz domains Ω : there is a positive constant C which depends only on Ω so that

$$(15) \quad \|\boldsymbol{\varepsilon}(\mathbf{u})\|_0 \geq C \|\mathbf{u}\|_1, \quad \forall \mathbf{u} \in \mathbf{H}.$$

This is a type of Korn's inequality. Combining this inequality and the derived inequality for $\tilde{a}(\cdot, \cdot)$ in [\(14\)](#) we obtain the coercivity of $\tilde{a}(\cdot, \cdot)$ in \mathbf{H} for non-axisymmetric domains:

$$(16) \quad \tilde{a}(\mathbf{u}, \mathbf{u}) \geq C^2 \min \left\{ 2\mu, d \left(\lambda + \frac{2\mu}{d}\right) \right\} \|\mathbf{u}\|_1^2, \quad \forall \mathbf{u} \in \mathbf{H}.$$

Provided Ω is a non-axisymmetric Lipschitz domain, the coercivity of $\tilde{a}(\cdot, \cdot)$ means that the solution operator $\tilde{T} : \mathbf{H} \rightarrow \mathbf{H}$ is well-defined, and satisfies

$$C^2 \min \left\{ 2\mu, d \left(\lambda + \frac{2\mu}{d}\right) \right\} \|\tilde{T}\mathbf{f}\|_1^2 \leq \tilde{a}(\tilde{T}\mathbf{f}, \tilde{T}\mathbf{f})_0 = (\mathbf{f}, \tilde{T}\mathbf{f}) \leq \|\tilde{T}\mathbf{f}\|_0 \|\mathbf{f}\|_0.$$

Furthermore,

$$(17) \quad \|\tilde{T}\mathbf{f}\|_1 \leq \frac{C^{-2}}{\min \left\{ 2\mu, d \left(\lambda + \frac{2\mu}{d}\right) \right\}} \|\mathbf{f}\|_l, \quad l \in \{0, 1\}, \forall \mathbf{f} \in \mathbf{H}.$$

Following [\[1\]](#), the compactness of the inclusion $\mathbf{H}^1(\Omega) \hookrightarrow \mathbf{L}^2(\Omega)$ and the previous bound with $l = 0$ imply the compactness of \tilde{T} . The Spectral Theorem for bounded self-adjoint linear and compact operators says that \tilde{T} has a countable real point spectrum

$\{\beta_n\} \subseteq (0, 1)$ and eigenfunctions $\{\mathbf{u}_n\}$ such that $\tilde{T}\mathbf{u}_n = \beta_n\mathbf{u}_n$ for all n . Note that (β_n, \mathbf{u}_n) solves Equation 13 if and only if \mathbf{u}_n solves Equation 11 with $\beta_n = \frac{1}{\kappa_n}$.

We remark that the results in this section also hold for the bilinear form $a(\cdot, \cdot)$ and therefore, since $\tilde{a}(\mathbf{u}, \mathbf{v}) = a(\mathbf{u}, \mathbf{v})$ for all $\mathbf{u}, \mathbf{v} \in \mathbf{H}$, this establishes the existence of the Jones spectrum for bounded Lipschitz domains Ω which are not axisymmetric.

In particular, this suggests that domains such as triangles and L-shaped domains should exhibit Jones modes. Since these are not available in closed form, we shall need to devise a suitable computational strategy for them.

3.2. The case of zero eigenvalues and rigid motions. When studying problems involving the Lamé operator \mathcal{L} , we need to be aware of rigid motions. Depending on the boundary conditions imposed, rigid motions may be part of the eigenspace of certain eigenvalues. Rigid motions satisfy $\mathcal{L}\mathbf{w} = \mathbf{0}$, and it is possible that they may satisfy both Equation 1b and Equation 1c. We now want to characterize domains having these eigenfunctions. Consider the space

$$\mathbf{RM}(\Omega) := \{\mathbf{u} \in \mathbf{H}^1(\Omega) : \mathbf{u} = \mathbf{b} + \mathbf{B}\mathbf{x}, \mathbf{b} \in \mathbb{R}^n, \mathbf{B} \in \mathbb{R}_{skew}^{n \times n}, \mathbf{x} \in \Omega\},$$

where $\mathbb{R}_{skew}^{n \times n}$ is the space of all skew-symmetric matrices in $\mathbb{R}^{n \times n}$. The space $\mathbf{RM}(\Omega)$ consists of translations, rotations and combinations of these. It is known that (see, e.g. [1] and references therein) the linear elasticity problem with traction boundary conditions

$$(18) \quad -\operatorname{div} \boldsymbol{\sigma}(\bar{\mathbf{u}}) = \delta \bar{\mathbf{u}}, \quad \text{in } \Omega, \quad \boldsymbol{\sigma}(\bar{\mathbf{u}})\mathbf{n} = \mathbf{0}, \quad \text{in } \partial\Omega,$$

has eigenmodes in $\mathbf{RM}(\Omega)$ with eigenvalue $\delta = 0$. In fact, if $n = 2$, the eigenspace of $\delta = 0$ is exactly $\mathbf{RM}(\Omega)$ with dimension 3. Define the space

$$\mathbf{Z} := \left\{ \mathbf{u} \in \mathbf{H}^1(\Omega) : \tilde{a}(\mathbf{u}, \mathbf{v}) = 0, \forall \mathbf{v} \in \mathbf{H}^1(\Omega) \right\}.$$

Examining the weak formulation of Equation 18, it is clear that $\mathbf{RM} \subseteq \mathbf{Z}$. We show that these spaces actually coincide.

LEMMA 3.1. *There holds $\mathbf{RM}(\Omega) = \mathbf{Z}$.*

Proof. First, let $\mathbf{u} \in \mathbf{RM}(\Omega)$. By definition, $\mathbf{u} = \mathbf{b} + \mathbf{B}\mathbf{x}$, $\mathbf{x} \in \Omega$, \mathbf{B} skew-symmetric. Then $\nabla \mathbf{u} = \mathbf{B}$ so that $\boldsymbol{\varepsilon}(\mathbf{u}) = \mathbf{0}$ and clearly $\tilde{a}(\mathbf{u}, \mathbf{v}) = 0$ for any $\mathbf{v} \in \mathbf{H}^1(\Omega)$. Conversely, assume $\mathbf{u} \in \mathbf{Z}$. Then $\tilde{a}(\mathbf{u}, \mathbf{u}) = 0$, and using the definition of $\tilde{a}(\cdot, \cdot)$ in Equation 12 we get

$$0 = 2\mu \operatorname{tr}(\boldsymbol{\varepsilon}(\mathbf{u})) + n\lambda \operatorname{tr}(\boldsymbol{\varepsilon}(\mathbf{u})) = n \left(\lambda + \frac{2}{n}\mu \right) \operatorname{tr}(\boldsymbol{\varepsilon}(\mathbf{u})).$$

Since $\lambda + \frac{2}{n}\mu > 0$, we get that both $\operatorname{tr}(\boldsymbol{\varepsilon}(\mathbf{u})) = 0$ and $\boldsymbol{\varepsilon}(\mathbf{u}) = \mathbf{0}$. This implies that $\mathbf{u} \in \mathbf{RM}(\Omega)$. \square

Now that we know the eigenvalue problem in Equation 18 has $\mathbf{RM}(\Omega)$ in the eigenspace of $\delta = 0$, the question is if there is any non-zero elements in $\mathbf{RM}(\Omega) \cap \mathbf{H}$, i.e., those which satisfy the additional constraint $\mathbf{u} \cdot \mathbf{n} = 0$ on the boundary. Such elements would be Jones modes corresponding to a zero Jones eigenvalue.

The next Lemma states the cases in which we have 2D rigid motions which additionally satisfy $\mathbf{u} \cdot \mathbf{n} = 0$ on the boundary. We note parts (i) and (ii) of the result can be combined for a more succinct statement involving arbitrary half-spaces, but state the version below for clarity of exposition.

LEMMA 3.2. *Assume $d = 2$. Then*

- (i) $\mathbf{RM}(\Omega) \cap \mathbf{H} = \text{span}\{(0, 1)^t\}$ if and only if $\Omega = \{(x_1, x_2)^t \in \mathbb{R}^2 : x_1 > a, x_2 \in \mathbb{R}\}$, for $a \in \mathbb{R}$.
- (ii) $\mathbf{RM}(\Omega) \cap \mathbf{H} = \text{span}\{(1, 0)^t\}$ if and only if $\Omega = \{(x_1, x_2)^t \in \mathbb{R}^2 : x_1 \in \mathbb{R}, x_2 > b\}$, for $b \in \mathbb{R}$.
- (iii) $\mathbf{RM}(\Omega) \cap \mathbf{H} = \text{span}\{(x_2, -x_1)^t\}$ if and only if $\Omega = B(0, R)$.

Proof. For (i), suppose $\Omega = \{(x_1, x_2)^t \in \mathbb{R}^2 : x_1 > a, x_2 \in \mathbb{R}\}$, for some $a \in \mathbb{R}$. Let $\mathbf{u} \in \mathbf{RM}(\Omega) \cap \mathbf{H}$. We write $\mathbf{u} = \mathbf{b} + \mathbf{B}\mathbf{x}$, $\mathbf{b} \in \mathbb{R}^2$, \mathbf{B} skew-symmetric, and $\mathbf{x} \in \Omega$. Assume

$$\mathbf{b} = (b_1, b_2)^t, \quad \mathbf{B} = \begin{pmatrix} 0 & b \\ -b & 0 \end{pmatrix}.$$

The normal on $\partial\Omega := \{(a, x_2) : x_2 \in \mathbb{R}\}$ is $\mathbf{n} = (-1, 0)^t$. We have

$$0 = \mathbf{u} \cdot \mathbf{n} = \mathbf{b} \cdot \mathbf{n} + \mathbf{B}\mathbf{x} \cdot \mathbf{n} = b_1 + bx_2, \quad \forall x_2 \in \mathbb{R}.$$

We must have $b_1 = 0$ and $b = 0$, which gives $\mathbf{B} = \mathbf{0}$ and $\mathbf{b} = (0, b_2)$, showing that $\mathbf{u} \in \text{span}\{(0, 1)^t\}$. Part (ii) can be easily proved by following the same steps showed before. For (iii), assume Ω is a circle of radius R centred at the origin. Let $\mathbf{u} \in \mathbf{RM}(\Omega) \cap \mathbf{H}$. As before, $\mathbf{u} = \mathbf{b} + \mathbf{B}\mathbf{x}$, $\mathbf{x} \in \Omega$, and $\mathbf{u} \cdot \mathbf{n} = 0$ on $\partial\Omega = \{(x_1, x_2) \in \mathbb{R}^2 : x_1^2 + x_2^2 = R^2\}$. Then

$$0 = \mathbf{u} \cdot \mathbf{n} = \mathbf{b} \cdot \mathbf{n} + \mathbf{B}\mathbf{x} \cdot \mathbf{n} = b_1n_1 + b_2n_2 + b(n_1x_2 - n_2x_1), \quad \forall (x_1, x_2) \in \partial\Omega.$$

The normal vector on $\partial\Omega$ is $\mathbf{n} = \frac{1}{R}(x_1, x_2)$. Putting this into the previous equation we obtain

$$b_1x_1 + b_2x_2 = 0, \quad \forall (x_1, x_2) \in \partial\Omega.$$

Since x_1 and x_2 cannot be zero simultaneously, we conclude that $b_1 = b_2 = 0$ and $\mathbf{u} = \mathbf{B}\mathbf{x}$, proving that $\mathbf{u} \in \text{span}\{(x_2, -x_1)^t\}$.

Note that the converse of all three parts (i), (ii) and (iii) are trivial since the basis of $\mathbf{RM}(\Omega) \cap \mathbf{H}$ is always orthogonal (in the Euclidean inner product) to the normal vector on the boundary of the corresponding domain. \square

In the lemma above one could also apply the results to the complement of each domain considered. Indeed, the complement of Ω in parts (i), (ii) and (iii), the normal vector only changes its sign, so the vanishing condition of the normal trace of the displacement would be readily satisfied in this case as well.

[Theorem 3.1](#) suggests that the traction eigenvalue problem given by [Equation 18](#) has zero as eigenvalue with eigenspace $\mathbf{RM}(\Omega)$. Moreover, $\mathbf{RM}(\Omega)$ is an eigenspace of the traction eigenproblem independent of the domain Ω . However, the extra constraint on the normal trace of the displacement \mathbf{u} (cf. [Equation 4](#)) may preclude 0 as a Jones eigenvalue on some domains. The elements in $\mathbf{RM}(\Omega) \cap \mathbf{H}$ depend on the boundary of Ω as shown in [Lemma 3.2](#). Combining [Lemma 3.1](#) and [Lemma 3.2](#), we have the following theorem.

THEOREM 3.3. *Suppose $\kappa = 0$ in [Equation 9](#) (equivalently [Equation 11](#)). We have:*

- (i) $\mathbf{u}_0 = (0, 1)^t$ is a Jones mode on $\Omega := \{(x_1, x_2)^t \in \mathbb{R}^2 : x_1 > a, x_2 \in \mathbb{R}\}$, for some $a \in \mathbb{R}$.

(ii) $\mathbf{u}_0 = (1, 0)^t$ is a Jones mode on $\Omega := \{(x_1, x_2)^t \in \mathbb{R}^2 : x_1 \in \mathbb{R}, x_2 > b\}$, for some $b \in \mathbb{R}$.

(iii) $\mathbf{u}_0 = (x_2, -x_1)^t$ is a Jones mode on $\Omega := B(0, R)$, for any fixed $0 < R < \infty$.

In the 3D case, a rigid motion can be decomposed as

$$\begin{aligned} \mathbf{u} = & c_1(1, 0, 0)^t + c_2(x_2, -x_1, 0)^t + c_3(x_3, 0, -x_1)^t + c_4(0, 1, 0)^t \\ & + c_5(0, x_3, -x_2)^t + c_6(0, 0, 1)^t, \end{aligned}$$

for constants $c_1, \dots, c_6 \in \mathbb{R}$. In this case, we see that we have three possible rotations and three possible translations. This implies that we may have more eigenvectors associated to the zero eigenvalue in [Equation 9](#) (equivalently [Equation 11](#)).

The spaces $\mathbf{T}(\Omega)$ and $\mathbf{R}(\Omega)$ are defined as the spaces of pure translations and pure rotations of Ω respectively. These allow the following decomposition of $\mathbf{RM}(\Omega)$:

$$\mathbf{RM}(\Omega) = \mathbf{T}(\Omega) \oplus \mathbf{R}(\Omega),$$

with trivial intersection. To characterize the elements of $\mathbf{RM}(\Omega) \cap \mathbf{H}$, it was shown in [\[3\]](#) that axisymmetric domains always support rotational displacements in \mathbf{R} which are tangential to the boundary.

3D versions of [Theorem 3.2](#) and [Theorem 3.3](#) can be now stated.

LEMMA 3.4. *Assume $d = 3$. Then*

- (i) $\mathbf{RM}(\Omega) \cap \mathbf{H} = \text{span}\{(1, 0, 0)^t\}$ if $\Omega := \{(x_1, x_2, x_3)^t \in \mathbb{R}^3 : bx_2 + cx_3 < a, x_1 \in \mathbb{R}\}$, for some $a, b, c \in \mathbb{R}$ such that $1 = b^2 + c^2$.
- (ii) $\mathbf{RM}(\Omega) \cap \mathbf{H} = \text{span}\{(0, 1, 0)^t\}$ if $\Omega := \{(x_1, x_2, x_3)^t \in \mathbb{R}^3 : ax_1 + cx_3 < b, x_2 \in \mathbb{R}\}$, for some $a, b, c \in \mathbb{R}$ such that $1 = a^2 + c^2$.
- (iii) $\mathbf{RM}(\Omega) \cap \mathbf{H} = \text{span}\{(0, 0, 1)^t\}$ if $\Omega := \{(x_1, x_2, x_3)^t \in \mathbb{R}^3 : ax_1 + bx_2 < c, x_3 \in \mathbb{R}\}$, for some $a, b, c \in \mathbb{R}$ such that $1 = a^2 + b^2$.
- (iv) $\mathbf{RM}(\Omega) \cap \mathbf{H} \subseteq \mathbf{R}(\Omega)$ if and only if Ω is axisymmetric.

Proof. (i), (ii) and (iii) readily follow by applying the same steps as in the proof of parts (i) and (ii) of [Theorem 3.2](#). For part (iv), let $\mathbf{u} \in \mathbf{RM}(\Omega) \cap \mathbf{H} \subseteq \mathbf{R}(\Omega)$, and assume Ω is a non-axisymmetric domain. Then, Korn's inequality (cf. inequality [\(15\)](#)) holds for \mathbf{u} , that is, there is a constant $c > 0$ such that $c\|\mathbf{u}\|_1 \leq \|\boldsymbol{\varepsilon}(\mathbf{u})\|_0$. However, $\mathbf{u} \in \mathbf{R}(\Omega)$ is a rotation so $\boldsymbol{\varepsilon}(\mathbf{u}) = \mathbf{0}$ and $\|\mathbf{u}\|_1 \neq 0$. This means that $c \leq 0$, which is a contradiction. For the converse of part(iv), assume that Ω is axisymmetric, and $\mathbf{R}(\Omega) \subseteq \mathbf{RM}(\Omega) \cap \mathbf{H}$ with strict inclusion. This implies there is an element of $\mathbf{RM}(\Omega) \cap \mathbf{H}$ which is a non-zero translation motion; however, the boundary condition on the normal trace prohibits such modes. \square

From here, [Theorem 3.1](#) and [Theorem 3.4](#) give the next result.

THEOREM 3.5. $\kappa = 0$ is an eigenvalue of [Equation 7](#) with eigenvector:

- (i) $\mathbf{u}_0 = (1, 0, 0)^t$ on $\Omega := \{(x_1, x_2, x_3)^t \in \mathbb{R}^3 : bx_2 + cx_3 < a, x_1 \in \mathbb{R}\}$, for some $a, b, c \in \mathbb{R}$ such that $1 = b^2 + c^2$.
- (ii) $\mathbf{u}_0 = (0, 1, 0)^t$ on $\Omega := \{(x_1, x_2, x_3)^t \in \mathbb{R}^3 : ax_1 + cx_3 < b, x_2 \in \mathbb{R}\}$, for some $a, b, c \in \mathbb{R}$ such that $1 = a^2 + c^2$.
- (iii) $\mathbf{u}_0 = (0, 0, 1)^t$ on the domain $\Omega := \{(x_1, x_2, x_3)^t \in \mathbb{R}^3 : ax_1 + bx_2 < c, x_3 \in \mathbb{R}\}$, for some $a, b, c \in \mathbb{R}$ such that $1 = a^2 + b^2$.
- (iv) $\mathbf{u}_0 \in \mathbf{R}(\Omega)$ whenever Ω is axisymmetric.

In the case of the circle in 2D, the zero eigenvalue would lead to a bilinear form $a(\cdot, \cdot)$ that is not \mathbf{H} -elliptic. For the 3D case, the axisymmetric domains would lead

to a loss of \mathbf{H} -ellipticity for the bilinear form $a(\cdot, \cdot)$. To overcome this issue, we add a shift to the formulation in Equation 9 to get the equivalent formulation: find $(\mathbf{u}, \kappa) \in \mathbf{H} \times \mathbb{C}$ such that

$$(19) \quad \bar{a}(\mathbf{u}, \mathbf{v}) = (\kappa + 1)(\mathbf{u}, \mathbf{v})_0, \quad \forall \mathbf{v} \in \mathbf{H},$$

with $\bar{a}(\mathbf{u}, \mathbf{v}) := a(\mathbf{u}, \mathbf{v}) + \rho(\mathbf{u}, \mathbf{v})_0$, for all $\mathbf{u}, \mathbf{v} \in \mathbf{H}$. This new formulation is obviously \mathbf{H} -elliptic since for any $\mathbf{u} \in \mathbf{H}$ we have

$$\bar{a}(\mathbf{u}, \mathbf{u}) = \mu \|\nabla \mathbf{u}\|_0^2 + (\lambda + \mu) \|\operatorname{div} \mathbf{u}\|_0^2 + \rho \|\mathbf{u}\|_0^2 \geq \min\{\mu, \rho\} \|\mathbf{u}\|_1^2.$$

The symmetry of $a(\cdot, \cdot)$ and the inner product $(\cdot, \cdot)_0$ along with the Rayleigh quotient (cf. (10)) show that the eigenvalues $\kappa + 1$ of Equation 19 are real and positive.

We define the solution operator $\bar{T} : \mathbf{H} \rightarrow \mathbf{H}$ by $\bar{T}\mathbf{f} = \mathbf{u}$ such that

$$(20) \quad \bar{a}(\mathbf{u}, \mathbf{v}) = (\mathbf{f}, \mathbf{v})_0, \quad \forall \mathbf{v} \in \mathbf{H},$$

Since $\bar{a}(\cdot, \cdot)$ is \mathbf{H} -elliptic, the Lax-Milgram lemma shows that \bar{T} is a well-defined linear operator and also gives the boundness of \bar{T} in the \mathbf{L}^2 - and \mathbf{H}^1 -norms:

$$(21) \quad \|\bar{T}\mathbf{f}\|_1 \leq \frac{1}{\min\{\mu, \rho\}} \|\mathbf{f}\|_l, \quad l \in \{0, 1\}, \quad \forall \mathbf{f} \in \mathbf{H}.$$

We again use the inclusion $\mathbf{H}^1(\Omega) \hookrightarrow \mathbf{L}^2(\Omega)$ is compact. Then, since \mathbf{H} is closed in $\mathbf{H}^1(\Omega)$, we have that \mathbf{H} is continuously embedded in $\mathbf{H}^1(\Omega)$, implying that the inclusion $\mathbf{H} \hookrightarrow \mathbf{L}^2(\Omega)$ is compact. This compact inclusion and the bound of \bar{T} in (21) with $l = 0$ imply that \bar{T} is a compact operator (see [1]). Also, the symmetry of $\bar{a}(\cdot, \cdot)$ implies that \bar{T} is a self-adjoint with respect to $\bar{a}(\cdot, \cdot)$. The Spectral Theorem for compact and self-adjoint bounded linear operators now implies the existence of eigenvalues $\{\alpha_n\}_{n \in \mathbb{N}} \subseteq (0, 1)$ and eigenfunctions $\{\mathbf{u}_n\}_{n \in \mathbb{N}}$ such that $\bar{T}\mathbf{u}_n = \alpha_n \mathbf{u}_n$ and $\alpha_n \rightarrow 0$. Note that $\bar{T}\mathbf{u}_n = \alpha_n \mathbf{u}_n$ is a solution of Equation 20 if and only if (κ_n, \mathbf{u}_n) solves Equation 9 with $\alpha_n := \frac{1}{\kappa_n + 1}$. We summarize these properties in the following main result.

THEOREM 3.6. *The point spectrum of \bar{T} is decomposed as follows: $\{\alpha_n\}_{n \in \mathbb{N}} \cup \{1\}$, where*

1. *the associated eigenspace of the eigenvalue 1 is given by Theorem 3.2 in 2D and Theorem 3.4 in 3D;*
2. *$\{\alpha_n\}_{n \in \mathbb{N}} \subseteq (0, 1)$ is a sequence of eigenvalues of \bar{T} with finite multiplicity that converges to 0 and their corresponding eigenfunctions lie in \mathbf{H} .*

We conclude this section by summarizing our main results. For axisymmetric domains, Jones modes exist and include 0 as an eigenvalue with certain rigid motions as permissible eigenmodes. For non-axisymmetric Lipschitz domains which are bounded, there are countably many positive Jones eigenvalues whose only accumulation point is at infinity.

4. Discretization. Let Ω be a polyhedral domain in \mathbb{R}^n , $n \in \{2, 3\}$. Let \mathcal{T}_h be a regular triangulation by triangles (or tetrahedra) of $\bar{\Omega}$ with mesh size h . For a given non-negative integer $k > 0$, we consider the space $\mathbf{P}_k(T)$ as the set of all vector polynomials of degree at most k defined on $T \in \mathcal{T}_h$. Define the space

$$\mathbf{H}_h := \left\{ \mathbf{v}_h \in C(\bar{\Omega}) : \mathbf{v}_h|_T \in \mathbf{P}_k(T), \quad \forall T \in \mathcal{T}_h \right\} \cap \mathbf{H},$$

and consider the problem: find $\mathbf{u}_h \in \mathbf{H}_h$ and $\kappa_h \in \mathbb{R}$ such that

$$(22) \quad a(\mathbf{u}_h, \mathbf{v}_h) = \kappa_h \cdot (\mathbf{u}_h, \mathbf{v}_h)_0, \quad \forall \mathbf{v}_h \in \mathbf{H}_h.$$

Besides, for non-axisymmetric domains, we have that the bilinear forms $\tilde{a}(\cdot, \cdot)$ and $a(\cdot, \cdot)$ coincides in \mathbf{H} . For these reasons, we only provide approximation results for the eigenvalue problem [Equation 9](#) as they readily apply to the formulations [Equation 11](#) and [Equation 19](#).

Since \mathbf{H}_h is a subspace of \mathbf{H} , the coercivity of $a(\cdot, \cdot)$ (cf. inequality [\(16\)](#)) in \mathbf{H} implies its \mathbf{H}_h -ellipticity. We can define a discrete solution operator T_h as follows:

$$\begin{aligned} T_h : \mathbf{H} &\rightarrow \mathbf{H}_h \\ \mathbf{f} &\rightarrow T_h \mathbf{f} := \mathbf{u}_h, \end{aligned}$$

where $\mathbf{u}_h \in \mathbf{H}_h$ is the solution of the problem

$$a(\mathbf{u}_h, \mathbf{v}_h) = (\mathbf{f}, \mathbf{v}_h) \quad \forall \mathbf{v}_h \in \mathbf{H}_h.$$

Once again, the pair (κ_h, \mathbf{u}_h) solves [Equation 22](#) if and only if $T_h \mathbf{u}_h = \sigma_h \mathbf{u}_h$ and $\sigma_h := \frac{1}{\kappa_h}$. Also, the restriction operator $T_h|_{\mathbf{H}_h} : \mathbf{H}_h \rightarrow \mathbf{H}_h$ is self-adjoint with respect to $a(\cdot, \cdot)$ and (\cdot, \cdot) . We have the following result concerning the spectrum of $T_h|_{\mathbf{H}_h}$ on polyhedron.

THEOREM 4.1. *Let Ω be a non-axisymmetric polyhedral domain. The spectrum of $T_h|_{\mathbf{H}_h}$ consists of $M_h := \dim(\mathbf{H}_h)$ eigenvalues, counted with their multiplicities.*

1. *The point spectrum consists of eigenvalues $\{\sigma_{h,k}\}_{k=1}^{M_h}$ in $(0, 1)$ counted with their multiplicities;*
2. *$\sigma_h = 0$ is not an eigenvalue of T_h .*

Concerning the approximation properties of this scheme, as described in [\[1\]](#), we have the following error bounds for the eigenvalues and eigenfunctions of [Equation 22](#):

$$(23) \quad \frac{|\kappa - \kappa_h|}{|\kappa|} \leq C\epsilon_h(\kappa)^2, \quad \|\mathbf{u} - \mathbf{u}_h\|_1 \leq C\epsilon_h(\kappa),$$

where the term ϵ_h is defined as

$$\epsilon_h(\kappa) := \sup_{\mathbf{u} \in \mathbf{H}(\kappa)} \inf_{\mathbf{u}_h \in \mathbf{H}_h} \|\mathbf{u} - \mathbf{u}_h\|_1.$$

For a given $\kappa \in \mathbb{C}$, the space $\mathbf{H}(\kappa)$ is a subspace of \mathbf{H} , given as

$$\mathbf{H}(\kappa) := \left\{ \mathbf{u} \in \mathbf{H} : \mathbf{u} \text{ solves } \text{Equation 9} \text{ with eigenvalue } \kappa, \|\mathbf{u}\|_0 = 1 \right\}.$$

That is, $\mathbf{H}(\kappa)$ is the eigenspace of the eigenvalue κ , containing normalized eigenvectors (in the \mathbf{L}^2 -norm).

The upper bounds for the errors in [Equation 23](#) hold for eigenvalues with multiplicity greater than 1. In fact, if κ is an eigenvalue of [Equation 9](#) of multiplicity $M \in \mathbb{N}$ with $\mathbf{u}_m \in \mathbf{H}(\kappa)$, for all $m = 1, \dots, M$, then there is a vector \mathbf{w} in the span $\{\mathbf{u}_1, \dots, \mathbf{u}_M\}$ and a vector field \mathbf{w}_h in the span of $\{\mathbf{u}_{1,h}, \dots, \mathbf{u}_{M,h}\}$ such that

$$\|\mathbf{w} - \mathbf{w}_h\|_1 \leq C\epsilon_h(\kappa),$$

where the vectors $\mathbf{u}_{1,h}, \dots, \mathbf{u}_{M,h}$ solve [Equation 22](#) with κ_h .

Regarding the approximation estimates of the finite element discretization, for a regular triangulation, the interpolation error estimate for the Lagrange finite elements is

$$\|\mathbf{u} - \mathbf{I}_h \mathbf{u}\|_s \leq Ch^{t-s} |\mathbf{u}|_t, \quad \forall \mathbf{u} \in \mathbf{H}^t(\Omega),$$

with \mathbf{I}_h is the vector version of the usual Lagrange interpolant (componentwise), $|\cdot|_t$ is the seminorm in $\mathbf{H}^t(\Omega)$, and $t, s > 0$. Using this interpolation error estimate in the error bound for κ in [Equation 23](#), we have

$$\frac{|\kappa - \kappa_h|}{|\kappa|} \leq ch^{2(t-1)} |\mathbf{u}|_t.$$

Note that the rate of convergence of the eigenvalues κ_h depends on the regularity of its corresponding eigenvector $\mathbf{u} \in \mathbf{H}^t(\Omega)$. Then computed eigenvectors would then decay as h^{t-1} .

5. Results. This last section presents some numerical results that support the theoretical findings provided in the previous sections.

5.1. Convergence studies for polyhedral domains. We show 4 numerical examples: 2 experiments on the square $\Omega_1 := [-1, 1]^2$, and 1 experiment on each of the following domains: L-shape $\Omega_2 := \Omega_1 \setminus (0, 1]^2$, and cube $\Omega_3 := [0, 1]^3$.

To summarize our results, consider the terms:

$$e_h(\kappa) := \frac{|\kappa - \kappa_h|}{|\kappa|}, \quad r(\kappa) := \frac{\log(e_h(\kappa)/e_{h'}(\kappa))}{\log(h/h')},$$

where \mathcal{T}_h and $\mathcal{T}_{h'}$ are two consecutive regular triangulations such that $h' < h$. In all the experiments we have used \mathbf{P}_1 -conforming elements to compute the approximated eigenpair on a sequence of regular (not necessarily uniform) meshes. The reference solution was computed with \mathbf{P}_2 -conforming elements on a very fine grid. These experiments were implemented in FreeFem++ [8]. It is important to remark that Dirichlet boundary conditions are added to the system as a penalty term.

On Ω_1 , we provide two different examples: one shows that the method reaches the predicted rate of convergence, while the second one shows how the assumptions on the Lamé constants influence the performance of this method. [Figure 2](#) shows how this approach fails when μ is close zero. The chosen parameters for this experiment are $\mu = 10^{-6}$, $\lambda = \rho = 1$. As expected, we can easily see that the approximation deteriorates in this case.

The convergence history of the first 5 eigenvalues of [Equation 9](#) on Ω_1 is shown in [Figure 4](#) top-left for the parameters set $\mu = 10$, $\lambda = 1$, $\rho = 12$. We observe that our method obtains a good convergence behaviour as we decrease the meshsize h . We can see that in all 5 cases the error goes down with a similar rate. In fact, [Table 1](#) shows that the rate of convergence of the 4-th eigenvalue $\kappa_{4,h}$ on Ω_1 is close to 2, as expected.

It is important to mention that the eigenvalues computed on Ω_1 have been compared with the true eigenvalues. It is easy to show that on a rectangle $[0, a] \times [0, b]$ with $a = b = 1$ the eigenvectors either satisfy a divergence free condition (compression modes) or a no rotation condition (shear modes). In this case the eigenvalues of [Equation 9](#) are given by $\kappa_{m\ell} = \rho w_{m\ell}^2$, (see [Equation 5](#) and [Equation 6](#))

$$w_{m\ell}^2 := \begin{cases} \frac{\mu}{\rho} \left(\left(\frac{m\pi}{a} \right)^2 + \left(\frac{\ell\pi}{b} \right)^2 \right), & \text{for shear modes,} \\ \frac{\lambda + 2\mu}{\rho} \left(\left(\frac{m\pi}{a} \right)^2 + \left(\frac{\ell\pi}{b} \right)^2 \right), & \text{for compression modes.} \end{cases}$$

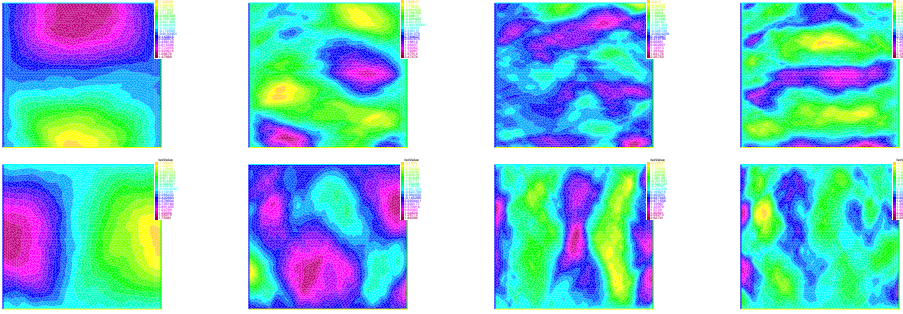


FIG. 2. x (top) and y (bottom) components of the 1st, 5th, 8th and 10th eigenfunctions (from left to right) on Ω_1 for small shear μ . The coercivity constant is very small in this case, impacting the quality of solutions as expected.

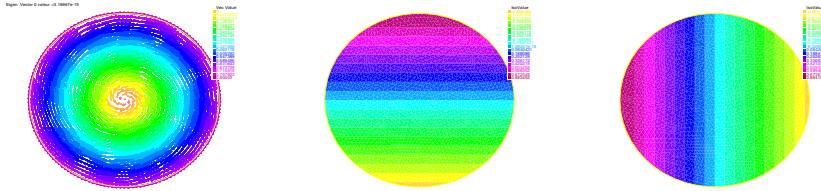


FIG. 3. Eigenfunction (left) $\mathbf{u}_{h,0}$, x -component (middle) and y -component (right) on the unit disk associated to the eigenvalue $\kappa_0 = 0$. The computations are performed on a grid comprising of triangles.

For our second example on the L-shaped domain Ω_2 , we set the parameters $\mu = \lambda = \rho = 1$. Here we expect to see a lack of convergence as one of the corners of the domain adds a singularity to the eigenfunctions. Indeed, Table 1 (second column) shows the rate of convergence of the $\kappa_{5,h}$ for the different refinements. We can see that the $r(\kappa_5)$ is below to one and oscillates around 1.7 through the different triangulations. This suggests that an a posteriori error analysis would be useful for these cases.

TABLE 1
Relative errors and rate of convergence for $\kappa_{4,h}$ on Ω_1 and for $\kappa_{5,h}$ on Ω_2 .

Ω_1			Ω_2		
h	$e(\kappa_4)$	$r(\kappa_4)$	h	$e(\kappa_5)$	$r(\kappa_5)$
0.56568	4.7368e-02	–	0.21483	2.5967e-01	–
0.32926	1.2742e-02	2.3286	0.15620	1.5176e-01	1.7120
0.20681	5.6958e-03	1.7624	0.10625	1.0798e-01	1.8181
0.14999	3.2038e-03	1.9461	0.083875	7.8904e-02	1.8368
0.12624	2.0903e-03	2.3232	0.063884	7.1002e-02	1.0594
0.10681	1.4788e-03	2.3173	0.058093	5.9216e-02	2.9458
0.090347	1.0486e-03	1.7994	0.046354	4.9365e-02	1.3221
0.080952	7.9184e-04	2.5311	0.042750	4.5914e-02	1.1815
0.075659	6.2612e-04	2.3573	0.039061	3.9448e-02	1.6733
0.068684	5.1616e-04	2.2290	0.035331	3.6429e-02	1.3534

5.2. Jones modes on a disk. If Ω is axisymmetric, the analysis in [subsection 3.2](#) implies that a shift needs to be added in [Equation 22](#). On the circle, a different discrete formulation to that for the previous subsection was used. The essential condition on the normal trace of the displacement is added to the formulation in [Equation 9](#). The equivalent mixed formulation would then be: find $(\mathbf{u}, p) \in \mathbf{H}^1(\Omega) \times H^1(\Omega)$ such that

$$\begin{aligned} \tilde{a}(\mathbf{u}, \mathbf{v}) + \langle \mathbf{v} \cdot \mathbf{n}, p \rangle_{1/2} &= \kappa \cdot (\mathbf{u}, \mathbf{v})_0, \quad \forall \mathbf{v} \in \mathbf{H}^1(\Omega), \\ \langle \mathbf{u} \cdot \mathbf{n}, q \rangle_{1/2} - \eta \cdot (p, q)_0 &= 0, \quad \forall q \in H^1(\Omega), \end{aligned}$$

where $\eta \geq 0$ is a stabilization constant. For $\eta = 0$, this formulation is obviously equivalent to [Equation 9](#). The stabilization term $\eta \cdot (p, q)_0$ is added only for implementation purposes as the Lagrange multiplier p is being defined on the whole domain Ω . Note that this implementation does not require the use of a penalty method to introduce Dirichlet boundary data as we needed for the original formulation [Equation 22](#). We present numerical results demonstrating this formulation on the disk, where we have used regular triangles. A full error analysis of this formulation on curvilinear domains will be presented in future work.

We consider the unit disk with parameters $\mu = 2$, $\lambda = 1$, and $\rho = 10$. As discussed in [subsection 3.2](#), an eigenmode associated to the eigenvalue $\kappa_0 = 0$ is added on the circle (2D case) as a consequence of the symmetry of the domain and the condition on the normal trace of the displacement on the boundary. [Figure 3](#) shows the eigenfunction \mathbf{u}_0 associated to κ_0 . We can see that this displacement is a rigid mode with a pure tangential displacement towards the boundary. Even though the boundary of Ω_3 is approximated by straight lines, the rate of convergence of the 4th eigenvalue, $r(\kappa_4)$, stays around 2 through the different triangulations (see first column in [Table 2](#)).

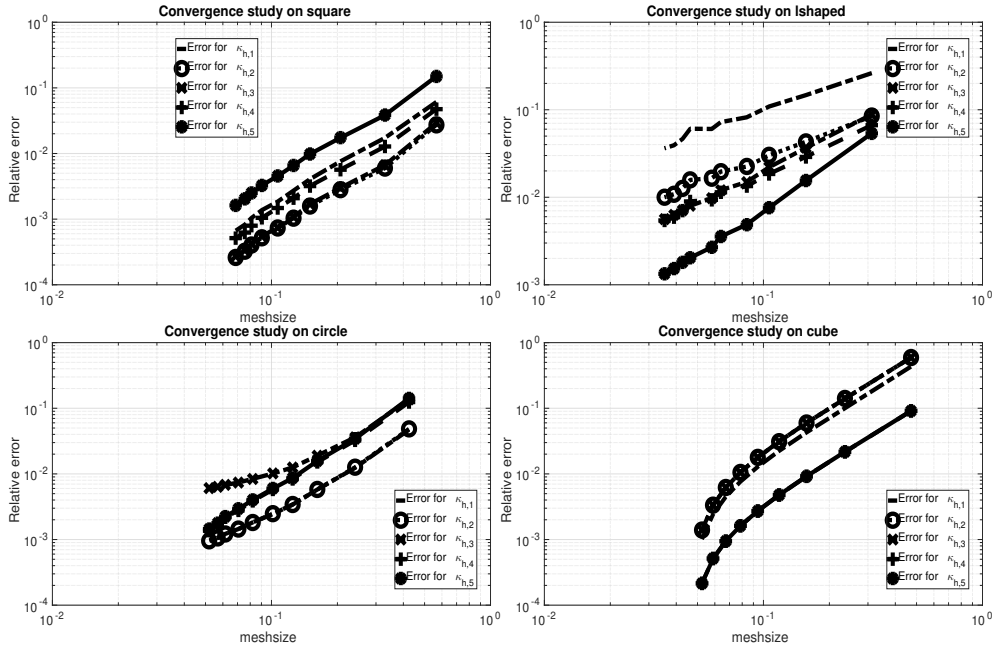


FIG. 4. Convergence study for the first 5 non-zero eigenvalues of [Equation 7](#) on Ω_1 (top-left), Ω_2 (top-right), Ω_3 (bottom-left) and Ω_4 (bottom-right).

In the last example on the unit cube Ω_4 with parameters $\mu = 10$, $\lambda = 1$, and $\rho = 12$. The second column of [Table 2](#) we show the rate of convergence of $\kappa_{2,h}$. We see that the rate is around 2 in most of the refinements. However, in some cases the rate is a bit higher than

TABLE 2
Relative errors and rate of convergence for $\kappa_{4,h}$ on the unit disk and for $\kappa_{2,h}$ on unit cube.

Ω_3			Ω_4		
h	$e(\kappa_4)$	$r(\kappa_4)$	h	$e(\kappa_2)$	$r(\kappa_2)$
0.42426	2.1564e-01	–	0.47140	3.9307e-01	–
0.24108	2.4728e-02	2.5077	0.23570	6.0195e-02	2.0775
0.16214	1.1095e-02	1.9561	0.15713	9.1960e-03	2.1132
0.12491	6.1557e-03	2.3125	0.11785	4.7800e-03	2.2593
0.10156	4.1815e-03	1.7727	0.094280	2.7333e-03	2.4931
0.082097	2.7884e-03	1.8946	0.078567	1.6205e-03	2.8586
0.070702	2.0222e-03	2.0846	0.067343	9.4898e-04	3.4642
0.061621	1.5580e-03	1.9359	0.058925	5.1297e-04	4.6015
0.056831	1.2003e-03	2.9146	0.052378	2.1394e-04	7.4204
0.052026	9.6266e-04	2.3241			

2. In fact, in the last three refinements we see that the rate of convergence is above 3 This was not expected at all for this discretization. Figure 4 (bottom right) plots the convergence history of the first 9 Jones eigenvalues on the unit cube. We notice that all the eigenvalues converge faster when the triangulation gets refined.

5.3. Examples of Jones modes. We end this section by using our discrete formulation to compute Jones modes on some geometries, to explore the dependence of the spectrum on domain shape and the Lamé parameters. We report also the L^2 norm of the divergence and rotational of the computed fields. In simple shapes the Jones modes can be readily identified as pure s - or p - modes. However, the eigenvalues can have multiplicity, and the eigenspaces may include eigenmodes of both types. This points to the need for care with resolving eigenmodes, as with any problem involving clusters.

As found in section 3, the Jones eigenvalue problem on Lipschitz domains possesses a countable set of eigenvalues $w_{m\ell}^2$, $m, \ell = 0, 1, 2, \dots$. For the sake of presentation, we set $\nu_j = w_{m\ell}^2$, with $j = j(m, \ell) \in \mathbb{N}_0$, such that $\nu_j \leq \nu_{j+1}$, for all $j \in \mathbb{N}_0$.

5.3.1. Square. We begin by observing that if $\lambda = 0$ and $\Omega = [0, 1]^2$ is the unit square, then the eigenmodes of Equation 1 are given analytically by setting $\lambda = 0$, $a = b = 1$ in Equation 5 and Equation 6. The eigenvalues are therefore of form

$$w_s^2 = \frac{\mu\pi^2}{\rho}(m^2 + \ell^2), \quad m, \ell > 0, \quad w_p^2 = \frac{2\mu\pi^2}{\rho}(m^2 + \ell^2), \quad m, \ell \geq 0, \quad m + \ell > 0.$$

If $\mu = \rho = 1$, the 4 initial eigenvalues ν_1, \dots, ν_4 (including multiplicity) are presented in Table 3. These eigenpairs were computed using our finite element method for this situation. We have also tabulated the L^2 -norm of the divergence and rotation of the eigenmodes; we see (modulo approximation error) that those eigenmodes are either pure s or p modes. The symmetry in the domain and the material parameters ensure $\nu_1 = \nu_2 = \nu_3$. We next consider the situation where $\mu = \rho = 1, \lambda = 2$ on the unit square. Due to the geometry, we see that $\nu_2 = \nu_3$. The eigenspace corresponding to the eigenvalues $\nu_6 = \nu_7$ will contain both a pure s - mode and a pure p - mode. This observation is borne out in Table 5; for a comparison with the same part of the spectrum for the case $\mu = \lambda = \rho = 1$ see Table 4.

5.3.2. Rectangle. We consider a rectangle of sides 1×2 . The asymmetry will affect the multiplicity of the eigenvalues, compared to the situation of the square.

In our first example, we set $\mu = \lambda = \rho = 1$. In contrast to the results in the square, this time the first three eigenvalues are simple. The numerically computed results are tabulated in Table 6. Increasing the shear μ to the value $\mu = 10$ while holding $\lambda = 1$ fixed does not impact the multiplicity of the initial eigenvalues, since this part of the spectrum includes

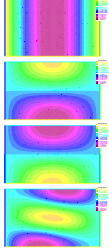
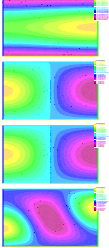
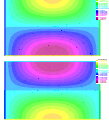
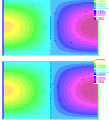
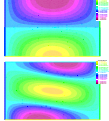
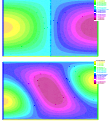
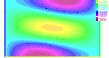
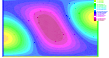
j	ν_j	ν_j/π^2	$\ \operatorname{div} \mathbf{u}\ _0^2$	$\ \operatorname{rot} \mathbf{u}\ _0^2$	x -component	y -component
1	19.74	2.000	9.870	0.0002633		
2	19.74	2.000	9.870	0.0001704		
3	19.74	2.000	5.883e-05	19.72		
4	39.48	4.000	19.74	0.0005061		

TABLE 3

Unit square with parameters $\mu = \rho = 1, \lambda = 0$.

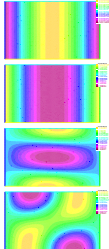
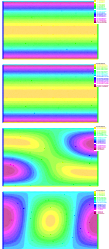
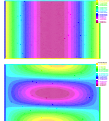
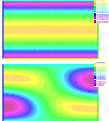
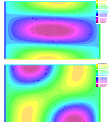
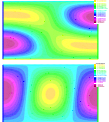
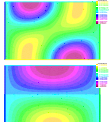
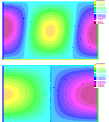
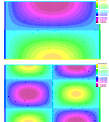
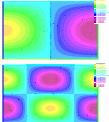
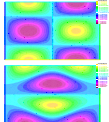
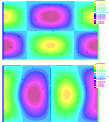
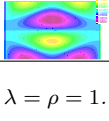
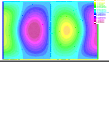
j	ν_j	ν_j/π^2	$\ \operatorname{div} \mathbf{u}\ _0^2$	$\ \operatorname{rot} \mathbf{u}\ _0^2$	x -component	y -component
1	19.74	2.000	5.048e-08	19.72		
2	29.61	3.000	9.870	0.000188		
3	29.61	3.000	9.870	0.0001293		
4	49.35	5.000	7.168e-07	49.22		
5	49.35	5.000	8.863e-07	49.25		
6	59.22	6.000	19.74	0.0005061		
7	78.96	8.000	2.979e-06	78.78		

TABLE 4

Unit square with parameters $\mu = \lambda = \rho = 1$.

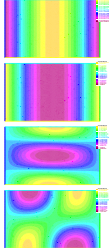
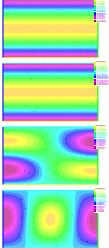
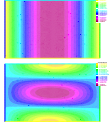
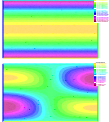
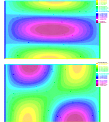
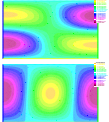
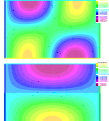
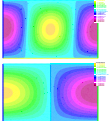
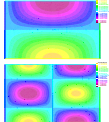
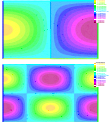
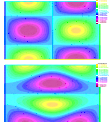
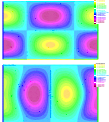
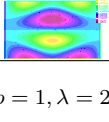
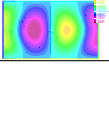
j	ν_j	ν_j/π^2	$\ \operatorname{div} \mathbf{u}\ _0^2$	$\ \operatorname{rot} \mathbf{u}\ _0^2$	x -component	y -component
1	19.74	2.000	5.048e-08	19.72		
2	39.48	4.000	9.870	0.000188		
3	39.48	4.000	9.870	0.0001294		
4	49.35	5.000	6.414e-07	49.22		
5	49.35	5.000	8.263e-07	49.25		
6	78.96	8.000	19.74	0.0005061		
7	78.96	8.000	2.742e-06	78.78		

TABLE 5

Unit square with parameters $\mu = \rho = 1, \lambda = 2$.

j	ν_j	ν_j/π^2	$\ \text{div } \mathbf{u}\ _0^2$	$\ \text{rot } \mathbf{u}\ _0^2$	x -component	y -component
1	7.402	0.750	2.467	2.271e-05		
2	12.34	1.250	2.053e-07	12.27		
3	19.74	2.000	1.592e-06	19.69		
4	29.61	3.000	9.869	0.0004004		

TABLE 6
 2×1 rectangle with parameters $\mu = \lambda = \rho = 1$.

both s - and p - modes (as in Table 7). On the other hand, fixing $\mu = 1$ and increasing λ to $\lambda = 10$ will affect the structure (s - or p - modes) of the initial eigenmodes, as can be seen in Table 8.

j	ν_j	ν_j/π^2	$\ \text{div } \mathbf{u}\ _0^2$	$\ \text{rot } \mathbf{u}\ _0^2$	x -component	y -component
1	51.82	5.25	2.467	2.271e-05		
2	123.4	12.5	2.271e-07	12.27		
3	197.4	20	1.757e-06	19.69		
4	207.3	21	9.869	0.0004004		
5	207.3	21	9.87	0.000243		

TABLE 7
 2×1 rectangle with parameters $\mu = 10, \lambda = \rho = 1$.

j	ν_j	ν_j/π^2	$\ \text{div } \mathbf{u}\ _0^2$	$\ \text{rot } \mathbf{u}\ _0^2$	x -component	y -component
1	12.34	1.250	1.231e-07	12.27		
2	19.74	2.000	9.515e-07	19.69		
3	29.61	3.000	2.467	2.271e-05		
4	32.08	3.250	2.74e-06	32.05		
5	41.95	4.250	2.223e-06	41.62		

TABLE 8
 2×1 rectangle with parameters $\mu = \rho = 1, \lambda = 10$.

5.4. L-shaped domain. The L-shaped domain discussed in the convergence studies does not have pure shear or pure compression Jones modes. This is due to the presence of the re-entrant corner (see Table 9). This example reveals, amongst other features, the need

to explore discretization strategies for the Jones eigenvalue problem which are able to handle low regularity.

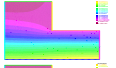
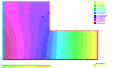
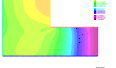
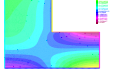
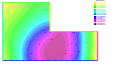
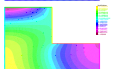
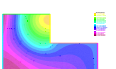
j	ν_j	ν_j/π^2	$\ \operatorname{div} \mathbf{u}\ _0^2$	$\ \operatorname{rot} \mathbf{u}\ _0^2$	x -component	y -component
1	0.08848	0.008965	0.01531	5.013		
2	1.285	0.1302	0.1411	5.273		
3	3.8100	0.3861	0.2903	15.43		
4	5.1300	0.5197	0.4458	8.277		

TABLE 9

L-shaped domain with parameters $\mu = \lambda = \rho = 1$.

5.5. Triangle. We finally present computed Jones eigenmodes on a isosceles triangle with vertices $(0, 0)$, $(2, 0)$ and $(0, 1)$. This triangle is not axisymmetric, and it is perhaps surprising (if entirely within the scope of our analysis) that this domain supports such modes. We choose $\lambda = \mu = \rho = 1$. As for the L-shaped domain, we do not see pure s - or p - modes as part of the eigenfunctions (see Table 10).

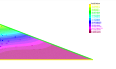
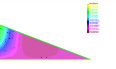
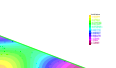
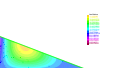
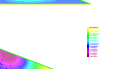
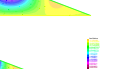
j	ν_j	ν_j/π^2	$\ \operatorname{div} \mathbf{u}\ _0^2$	$\ \operatorname{rot} \mathbf{u}\ _0^2$	x -component	y -component
1	4.6563	0.4718	0.7007	24.36		
2	8.3125	0.8422	0.4333	14.42		
3	11.84674	1.200	2.527	4.15		
4	21.0647	2.134	1.640	75.96		

TABLE 10

Isosceles triangle of vertices $(0, 0)$, $(2, 0)$ and $(1, 2)$ with parameters $\lambda = \mu = \rho = 1$.

6. Conclusions. We presented results establishing the existences of Jones modes on Lipschitz domains. The spectrum of the depends heavily on the shape of the domain we consider (as shown in section 3), adding more eigenpairs in the case of, for example axisymmetric domains. We presented also a finite element strategy for computing these eigenpairs. The FEM performs well for polyhedral domains. The situation for axisymmetric domains particularly with smooth boundary is more challenging, and subject for future work.

Acknowledgements. Sebastian Dominguez thanks the support of CONICYT-Chile, through Becas Chile. Nilima Nigam gratefully thanks the financial support of the National Sciences and Engineering Research Council of Canada (NSERC) Discovery Grants. The research of Jiguang Sun was partially supported by NSF grant DMS-1521555.

REFERENCES

- [1] I. BABUSKA AND J. OSBORN, *Eigenvalue problems*, Handbook of Numerical Analysis, 2 (1991), pp. 641–787, [https://doi.org/10.1016/S1570-8659\(05\)80042-0](https://doi.org/10.1016/S1570-8659(05)80042-0).
- [2] H. BARUCQ, R. DJELLOULI, AND E. ESTECAHANDY, *On the existence and the uniqueness of the solution of a fluidstructure interaction scattering problem*, Journal of Mathematical Analysis and Applications, 412 (2014), pp. 571 – 588, <https://doi.org/https://doi.org/10.1016/j.jmaa.2013.10.081>.
- [3] S. BAUER AND D. PAULY, *On korn's first inequality for tangential or normal boundary conditions with explicit constants*, Mathematical Methods in the Applied Sciences, 39, pp. 5695–5704, <https://doi.org/10.1002/mma.3954>, <https://onlinelibrary.wiley.com/doi/abs/10.1002/mma.3954>, <https://arxiv.org/abs/https://onlinelibrary.wiley.com/doi/pdf/10.1002/mma.3954>.
- [4] S. C. BRENNER, *Korn's inequalities for piecewise h_1 / h_2 vector fields*, Mathematics of Computation, 73 (2004), pp. 1067–1087, <http://www.jstor.org/stable/4099887>.
- [5] L. DESVILLETES AND C. VILLANI, *On a variant of korn's inequality arising in statistical mechanics*, ESAIM: Control, Optimisation and Calculus of Variations, 8 (2002), p. 603619, <https://doi.org/10.1051/cocv:2002036>.
- [6] G. N. GATICA, G. C. HSIAO, AND S. MEDDAHI, *A residual-based a posteriori error estimator for a two-dimensional fluid–solid interaction problem*, Numerische Mathematik, 114 (2009), pp. 63–106, <https://doi.org/10.1007/s00211-009-0250-6>, <https://doi.org/10.1007/s00211-009-0250-6>.
- [7] T. HARGÉ, *Valeurs propres d'un corps élastique*, Comptes rendus de l'Académie des sciences. Série 1, Mathématique, 311 (1990), pp. 857–859.
- [8] F. HECHT, *New development in freefem++*, Journal of numerical mathematics, 20 (2012), pp. 251–266, <https://doi.org/https://doi.org/10.1515/jnum-2012-0013>.
- [9] L. HENG WANG, *On korn's inequality*, Journal of Computational Mathematics, 21 (2003), pp. 321–324, <http://www.jstor.org/stable/43693072>.
- [10] C. O. HORGAN, *Korn's inequalities and their applications in continuum mechanics*, SIAM Rev., 37 (1995), pp. 491–511, <https://doi.org/10.1137/1037123>, <https://doi.org/10.1137/1037123>.
- [11] G. C. HSIAO, R. E. KLEINMAN, AND G. F. ROACH, *Weak solutions of fluidsolid interaction problems*, Mathematische Nachrichten, 218 (2000), pp. 139–163, [https://doi.org/10.1002/1522-2616\(200010\)218:1\(139::AID-MANA139\)3.0.CO;2-S](https://doi.org/10.1002/1522-2616(200010)218:1(139::AID-MANA139)3.0.CO;2-S).
- [12] G. C. HSIAO AND N. NIGAM, *A transmission problem for fluid-structure interaction in the exterior of a thin domain*, Adv. Differential Equations, 8 (2003), pp. 1281–1318.
- [13] G. C. HSIAO, T. SÁNCHEZ-VIZUET, AND F.-J. SAYAS, *Boundary and coupled boundaryfinite element methods for transient wavestructure interaction*, IMA Journal of Numerical Analysis, 37 (2017), pp. 237–265, <https://doi.org/10.1093/imanum/drw009>.
- [14] T. HUTTUNEN, J. P. KAIPIO, AND P. MONK, *An ultra-weak method for acoustic fluid-solid interaction*, J. Comput. Appl. Math., 213 (2008), pp. 166–185, <https://doi.org/10.1016/j.cam.2006.12.030>, <https://doi.org/10.1016/j.cam.2006.12.030>.
- [15] D. S. JONES, *Low-frequency scattering by a body in lubricated contact*, The Quarterly Journal of Mechanics and Applied Mathematics, 36 (1983), pp. 111–138, <https://doi.org/10.1093/qjmam/36.1.111>.
- [16] R. J. KNOPS AND L. E. PAYNE, *Uniqueness theorems in linear elasticity*, Springer-Verlag, New York-Berlin, 1971. Springer Tracts in Natural Philosophy, Vol. 19.
- [17] H. LAMB, *On the Vibrations of an Elastic Sphere*, Proc. Lond. Math. Soc., 13 (1881/82), pp. 189–212, <https://doi.org/10.1112/plms/s1-13.1.189>, <https://doi.org/10.1112/plms/s1-13.1.189>.
- [18] C. J. LUKE AND P. A. MARTIN, *Fluid-solid interaction: acoustic scattering by a smooth elastic obstacle*, SIAM J. Appl. Math., 55 (1995), pp. 904–922, <https://doi.org/10.1137/S0036139993259027>, <https://doi.org/10.1137/S0036139993259027>.
- [19] P. A. MARTIN, *Shear-wave resonances in a fluid-solid-solid layered structure*, Wave Motion, 51 (2014), pp. 1161–1169, <https://doi.org/10.1016/j.wavemoti.2014.07.002>, <http://dx.doi.org/10.1016/j.wavemoti.2014.07.002>.
- [20] S. MEDDAHI, D. MORA, AND R. RODRÍGUEZ, *Finite element spectral analysis for the mixed formulation of the elasticity equations*, SIAM Journal on Numerical Analysis, 51 (2013), pp. 1041–1063, <https://doi.org/10.1137/120863010>.
- [21] D. NATROSHVILI, G. SADUNISHVILI, AND I. SIGUA, *Some remarks concerning Jones eigenfrequencies and Jones modes*, Georgian Math. J., 12 (2005), pp. 337–348.
- [22] J. A. NITSCHKE, *On korn's second inequality*, ESAIM: Mathematical Modelling and Numerical

Analysis - Modlisation Mathmatique et Analyse Numrique, 15 (1981), pp. 237–248, <http://eudml.org/doc/193380>.